Fourier Transform Infrared Spectroscopy in Colloid and Interface Science

David R. Scheuing, EDITOR
Clorox Technical Center

Developed from a symposium sponsored
by the Division of Colloid and Surface Chemistry
of the American Chemical Society
at the 199th National Meeting
Boston, Massachusetts, April 22–27, 1990

American Chemical Society, Washington, DC 1990

Chapter 11

Monolayer Structure at Gas–Liquid and Gas–Solid Interfaces

Infrared Reflectance Spectroscopy as a Probe

Richard A. Dluhy[1] and Donald G. Cornell[2]

[1]Department of Chemistry, School of Chemical Sciences, University of Georgia, Athens, GA 30602
[2]Agricultural Research Service, U.S. Department of Agriculture, 600 E. Mermaid Lane, Philadelphia, PA 19118

Within recent years, external reflection-absorbance infrared spectroscopy has been adapted to the study of conformation-sensitive vibrational modes in amphiphilic monolayers at non-metallic surfaces. Included in this group is the class of monomolecular films that form ordered two-dimensional arrays at the air-water (A/W) interface. It has proven possible to investigate the surface-induced first order thermodynamic phase transition of phospholipid monolayer films at the A/W interface using this technique. Results of this work have focused on describing the nature of the phase transition, the design of an automated Langmuir-type film balance and its interfacing to the spectrometer, and the construction of a model to describe the orientation of the vibrational dipole moments based on the polarized reflectance spectra. In addition, the ability to probe the A/W interface allows us to directly compare the IR spectra of *in-situ* monolayers with the spectra of monolayer films transferred to attenuated total reflectance (ATR) crystals using classical Langmuir-Blodgett techniques, in order to determine whether the physical process of transfer disrupts the structure of the monolayer film.

During the decade of the 1980's, the discipline of surface and interfacial science has encountered tremendous growth. Organized two-dimensional organic films at interfaces have become an important component in a wide variety of disciplines, including non-linear optics, sensor applications, catalysis, surface modification, electrode coatings, and biomacromolecules (*1*). Surface chemistry has also benefited from the development of modern, sensitive spectroscopic techniques that have enabled investigators to study monomolecular films at interfaces spectroscopically for the first time. Table I lists many of the spectroscopic methods that are currently used to study surface and interfaces; several of these techniques were only first developed during the 1980's.

Table I. Spectroscopic Techniques Used For Surface Characterization

Ion Spectroscopy	Electron Spectroscopy
• Secondary Ion MS	• Low Energy Electron Diffraction
• Laser Microprobe MS	• X-Ray Photoelectron
• Particle-Induced X-Ray Emission	• Auger Electron
• Ion Scattering	• Electron Energy Loss
• Rutherford Backscattering	
Microscopic Techniques	**X-Ray Techniques**
• Electron	• Glancing Angle X-Ray Diffraction
• Scanning Tunneling	• Appearance Potential
• Atomic Force	• Extended X-Ray Fine Structure
Desorption Techniques	**Optical Spectroscopy**
• Electron Stimulated Desorption	• Fluorescence
• Laser-Induced Desorption	• UV-VIS
• Thermal Desorption	• Circular Dichroism
	• Quasi-Elastic Light Scattering
	• Brillouin Scattering
	• Second Harmonic Generation
	• Sum Frequency Generation
	• Raman
	• Infrared

Most of the contemporary research areas that utilize surface chemistry techniques employ thin organic films that have been physically or chemically adsorbed onto a solid (usually metallic) substrate. The use of conducting metal surfaces is due not only to their relevance to many different fields, but also to the fact that many surface spectroscopic techniques (Table I) need such a surface in order to produce high-quality spectra. This criterion effectively eliminated many interesting non-metallic surfaces from study using modern surface-sensitive spectroscopic methods.

However, continuing development of spectroscopic sampling techniques in recent years has increasingly led to the use of non-metallic surfaces as thin-film substrates, and the structure of the adsorbed film on these surfaces is now being elucidated via spectroscopic techniques. Included in this group is the class of

monomolecular films that form ordered two-dimensional arrays at the air-water (A/W) interface (a full list of abbreviations used in this chapter appears at the end before the literature citations). Insoluble monolayers at the A/W interface have been extensively studied as models for ionic, dipolar, and interfacial phenomena in systems such as surfactants, polymers, proteins, steroids, membranes, and other biophysical systems. The usefulness of these monolayers stems from the fact that the experimenter is able to dynamically change the physical state of the film during the experiment; in addition interfacial interactions can be probed in real time.

Unfortunately, while insoluble monolayers at the A/W interface have been extensively studies as models for interfacial phenomena, there is virtually no information available concerning the detailed physical structure of these films. Historically, this lack of information concerning the molecular-level structure of monolayers at the A/W interface can be traced to the inability of most spectroscopic techniques to study a low surface area, flat water interface with sufficient sensitivity to produce spectra with reasonable signal-to-noise ratios. This situation is changing with the introduction of the modern spectroscopic methods mentioned above. Even here, however, the number of spectroscopic techniques with *in-situ* sensitivity at the A/W interface is not large. Table II lists the methods that have been recently utilized to study the A/W interface *in-situ*.

Table II. Spectroscopic Techniques Used For In-Situ Characterization at the A/W Interface

X-Ray Techniques

- Glancing Angle X-Ray Diffraction

Optical Spectroscopy

- Fluorescence
- Quasi-Elastic Light Scattering
- Second Harmonic Generation
- Sum Frequency Generation
- Resonance Raman
- Infrared Reflectance

From a practical standpoint, the use of the glancing angle X-ray method, while powerful, requires a synchrotron source and therefore, due to the constraints of beam time, is necessarily limited in the number of systems that can be studied in a given time period. Of the optical methods listed, the fluorescence and resonance Raman techniques directly measure spectra of an embedded

chromophore, and thus give only indirect information concerning the host monolayer. The second harmonic methods (i.e. second harmonic and sum frequency generation) have the advantage of being uniquely surface-sensitive, however, they are limited to visible detection in the case of second harmonic generation, and suffer from insufficient spectral sensitivity. In contrast, the infrared reflectance method, as we have shown (*2-6*), is able to give direct information on the structure of the monolayer without the use of probe molecules. In addition, the infrared reflectance technique is highly surface-sensitive, due to the fact that vibrational spectroscopy measures changes in the dipole moment of specific chemical groups in the molecule.

Experimental Methods

Materials. 1,2-Dipalmitoyl-*sn*-glycero-3-phosphocholine (DPPC) was obtained from Avanti Polar Lipids, Inc. (Birmingham, AL) at 99% stated purity. The DPPC was further purified by dissolving it in dry, glass-distilled $CHCl_3$ and reprecipitating the lipid from dry, glass-distilled acetone (5:95 $CHCl_3$:acetone v/v). The precipitate was allowed to cure for one hour under refrigeration before centrifugation. This procedure was repeated six times.

Monolayer Film Preparation. Phospholipid monolayers for the *in-situ* infrared reflectance experiments were formed on the surface of an all-Teflon automated Langmuir film balance, the detailed design of which has been previously reported (*3*). The demountable trough was prepared for each experiment by cleaning with chromic acid cleaning solution, followed by exhaustive water rinsing. Sub-phase water was prepared from a Milli-Q ion exchange system (Millipore Inc., Bedford, MA) and had a nominal resistivity of 18 mega-ohm/cm. Temperature control of the subphase was established by thermostatting the hollow aluminum base plate on which the trough was mounted. The subphase temperature for the experiments reported here was 22 ± 1 °C. DPPC monolayer films were prepared by spreading from a 1 mg ml^{-1} lipid solution in n-hexane/ethanol (9:1 v/v) onto the A/W interface; the monolayer film was then allowed to equilibrate for ten minutes before the start of data collection. Surface pressure was monitored by use of a filter paper Wilhelmy plate (GVWP, 0.22 μm, Millipore Corp.), which was suspended from an electronic microbalance (Model 27, Cahn Inc., Cerritos, CA). The calculation of surface pressure and molecular area for the pure DPPC monolayer film using these experimental conditions has been described earlier (*3*).

Infrared Spectroscopy of Monolayer Films. External reflectance IR spectra of the DPPC monolayer film at the A/W interface were obtained using a Digilab FTS-40 FT-IR spectrometer (Digilab, Inc., Cambridge, MA). The IR spectra were collected using 1024 scans at 8 cm^{-1} resolution with triangular apodization, one level of zero-filling, and a narrow-band, liquid-N_2-cooled HgCdTe detector. The incoming radiation was polarized using an IR polarizer (Al wire grid on KRS-5, from Cambridge Physical Sciences); the polarizer was placed in the optical path between the spectrometer and the water surface. For both parallel and perpendicular polarizations, external reflection-absorbance spectra were obtained by ratioing (in

absorbance mode) the single beam reflectance spectrum of the monolayer-covered H_2O surface to the single beam reflectance spectrum of pure H_2O which served as the background. Monolayer IR spectra were obtained as a function of surface pressure by compression of the Langmuir film balance barriers until the desired surface pressure was obtained; compression was then stopped during data collection. A barrier compression rate of 0.20 cm min^{-1} was used. Frequencies and intensities of the CH_2 stretching modes were calculated using a center-of-gravity algorithm (*7*); the frequencies of the stretching bands calculated using this method are estimated to be accurate to greater than ± 0.1 cm^{-1}.

Transferred Monolayers. A separate film balance and trough was used for the preparation of Langmuir-Blodgett (L-B) monolayers transferred onto solid substrates. The design of this film balance has been described in detail elsewhere (*8*). The L-B monolayers were transferred onto germanium ATR crystals (50x10x2 mm, 45° face angle, obtained from Wilmad Glass Company, Buena, NJ). The film balance used for external reflection IR analysis and the film balance used for transferred films both employed Wilhelmy plates and dual compression barriers driving toward the center of the trough. In the preparation of transferred films, the Ge crystal was located centrally between the compression barriers; hence, there was no net movement of the film either at the point where transfer was effected or where the external reflection IR data was obtained. Monolayer films to be transferred were prepared in a manner similar to those used for external reflection IR analysis. After the phospholipid was spread, the solvent was allowed to evaporate for 15 minutes. Compression was begun and proceeded until the desired pressure was reached; transfer was then immediately started. The process of film transfer onto the 50 mm Ge crystal was accomplished with the aid of a rack and pinion device and took approximately 2 minutes. Constant film pressure was maintained during transfer by a microprocessor-controlled feedback loop (*8*).

Results and Discussion

Monolayer Films at the A/W Interface. Previous studies of phospholipid monolayers at gas-liquid interfaces have shown that it is possible to follow the first order thermodynamic phase transition of these monolayer films using the infrared reflectance techniques described in this manuscript (see e.g. ref. *6* and references cited therein). For long chain hydrocarbon molecules, it has been demonstrated that the frequencies of the antisymmetric and symmetric CH_2 stretching vibrations are conformation-sensitive, and may be empirically correlated with the order (i.e. the trans-gauche character) of the hydrocarbon chains (*9-11*).

Figure 1 demonstrates such a correlation between the surface pressure of a DPPC monolayer film (Figure 1A) and the frequency of the antisymmetric CH_2 stretching vibration (Figure 1B), both measured as a function of molecular area. Four phases are generally described in the pressure-area curve: the liquid-expanded (LE) region (> ca. 76 $Å^2$ $molecule^{-1}$), the main liquid-expanded to liquid-condensed (LE-LC) transition region (~55-76 $Å^2$ $molecule^{-1}$), the liquid-condensed to solid-condensed (LC-SC) region (~40-55 $Å^2$ $molecule^{-1}$) and the collapsed (C) film (< ca. 40 $Å^2$ $molecule^{-1}$). The observed band frequency decreases (i.e. the hydrocarbon chains become more ordered) as the molecular area decreases. Previous studies

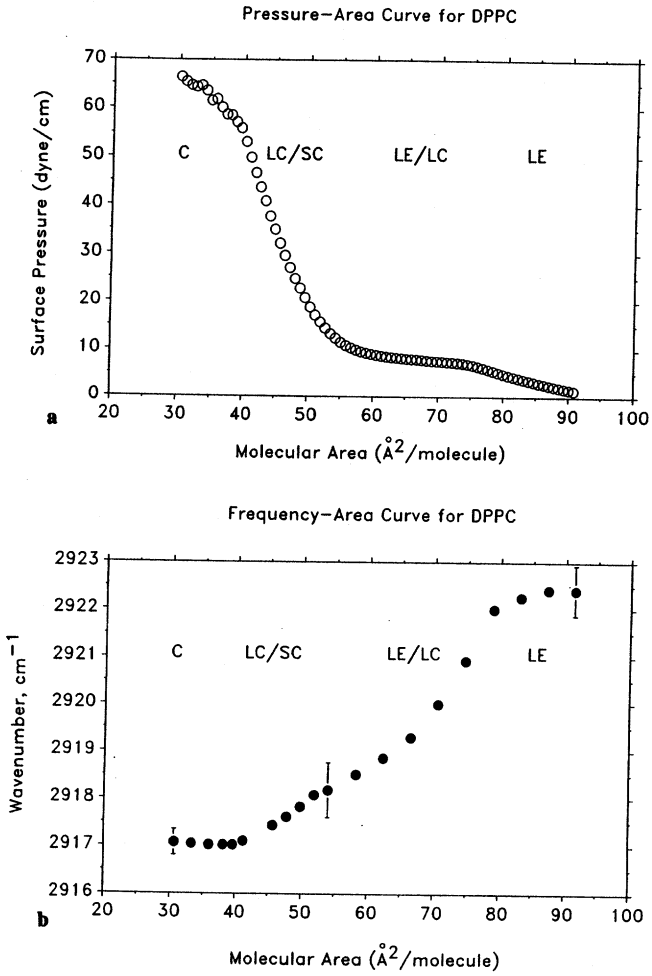

Figure 1. The surface pressure-molecular area isotherm of the DPPC monolayer at 22 °C (Figure 1A, top) with the infrared frequencies of the CH_2 antisymmetric stretching vibration, plotted against molecular area for the DPPC monolayer (Figure 1B, bottom).

have described this frequency decrease in terms of the thermodynamic state of the monolayer film (*6*). The large decrease ($\sim$3 cm^{-1}) in frequency between 55 $Å^2$ and 75 $Å^2$ is related to the first-order thermodynamic phase transition of the monolayer. In addition, a second, smaller decrease ($\sim$1 cm^{-1}) in frequency is noted between 40 $Å^2$ and 50 $Å^2$. This frequency shift is not related to the previous phase transition, but rather occurs in the condensed region of the pressure-area diagram where the monolayer film surface pressure begins to rise sharply. This frequency shift can be attributed to a further ordering of the lipid hydrocarbon chains beyond that observed during the main transition. Recent synchrotron X-ray diffraction results also report the appearance of more solid domains in the condensed region of monolayer films of 1,2-dimyristoyl-*sn*-glycero-3-phosphatidic acid (*12*). This second transition is assigned to a change in the packing of the hydrocarbon chains upon further film compression and is analogous to a solid-solid type hydrocarbon transition.

In addition to describing the conformation of the hydrocarbon chains for amphiphilic molecules at the A/W interface, external reflectance infrared spectroscopy is also capable of describing the orientation of the acyl chains in these monolayers as a function of the monolayer surface pressure. The analysis of the orientation distribution for an infrared dipole moment at the A/W interface proceeds based on classical electromagnetic theory of stratified layers (*2*). In particular, when parallel polarized radiation interacts with the A/W interface, the resultant standing electric field has contributions from both the z component of the p-polarized radiation normal to the interface, as well as the x component of the p-polarized radiation in the plane of the interface. The E field distribution for these two components changes based on the incoming angle of incidence of the p-polarized radiation. A geometrical representation of the incoming radiation as well as the resulting mean square electric fields for the A/W interface are shown in Figure 2.

The theoretical absorbances for a monolayer at the A/W interface may be calculated by taking into account this change of E field distribution as a function of the angle of incidence of the incoming radiation. Figure 3 is an example of such a theoretical absorbance calculation for a monolayer film at the A/W interface. In the calculation of Figure 3 it was assumed that the monolayer was 25 Å in thickness, with optical constants of n=1.5, k=0.1. The optical constants of H_2O were taken at 3000 cm^{-1} (*13*). The behavior of the p-polarized absorbance shows the previously-reported (*2*) discontinuity at $\sim$54° (the value for the Brewster angle of the A/W interface). Below 54°, the expected p-polarized absorbance is negative; above 54° the expected absorbance is positive. Figure 3 also indicates that for s-polarized radiation, the expected absorbances are negative regardless of the incoming angle of incidence.

Figures 4A and 4B present experimental spectra that illustrate the principle that the incoming E field distribution helps govern the type of spectra obtained. In Figure 4A, spectra of a DPPC monolayer are presented which were obtained at 60 ° angle of incidence with s-polarized radiation. As in previous studies where the experimental angle of incidence was 30° (*2-6*), the observed spectra have negative absorbances. In Figure 4B, however, the spectra of the monolayer taken with p-polarized radiation show positive absorbance bands, as predicted from theory (Figure 3).

In the case of external reflectance at air-metal surfaces, the resultant standing E field has a contribution solely due to the z component of the p-polarized light; the

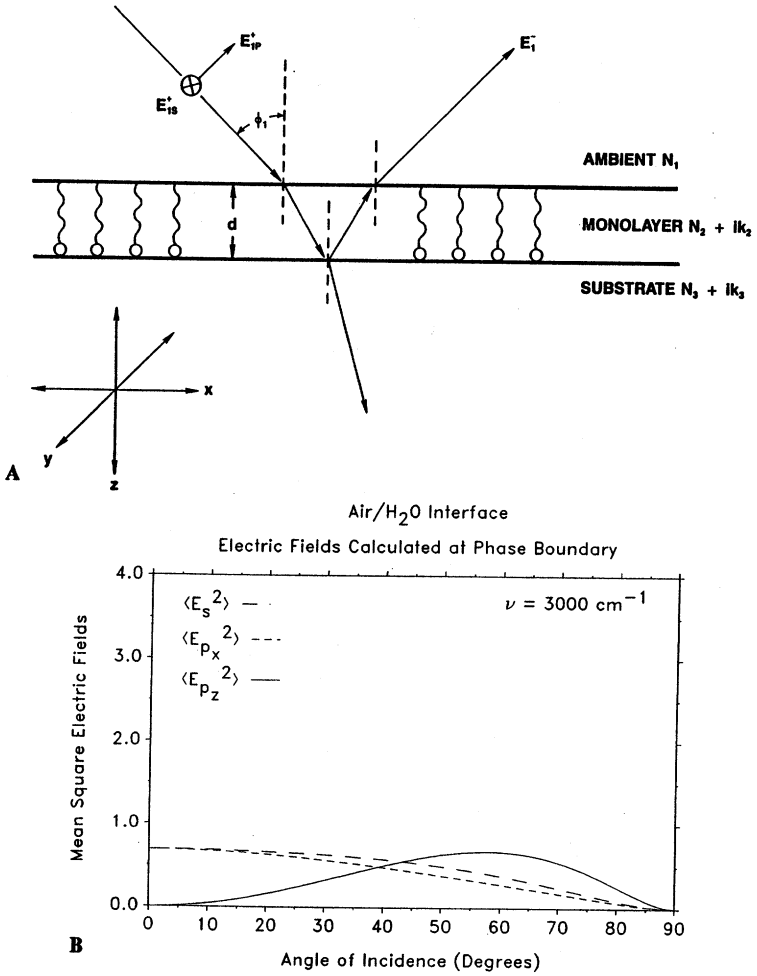

Figure 2. (A) Schematic illustration of the interaction of a plane electromagnetic wave in a three-phase system. Parallel (p) and perpendicular (s) components are shown for the incoming propagating wave (+ superscript). The coordinate geometry is indicated in the lower left of the diagram. (B) The mean-square electric field intensities at the A/W interface vs. the angle of incidence of the incoming plane wave. The optical parameters are: $n_1=1.0$; $n_2=1.441$, $k_2=0.0297$, at 3000 cm^{-1}. The magnitude shown is relative to that of the incident beam (defined as 1.0). (Figure 2A reproduced with permission from Reference 2. Copyright 1986 American Chemical Society. Figure 2B adapted from Reference 2).

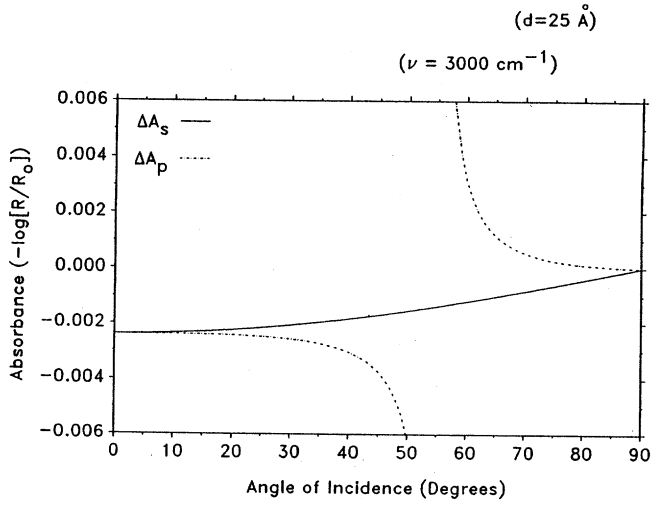

Figure 3. Theoretical absorbance for a monolayer at the A/W interface plotted as a function of the experimental angle of incidence of the incoming radiation. The solid line indicates the theoretical absorbance for s-polarized radiation; the dashed line indicates the theoretical absorbance for p-polarized radiation.

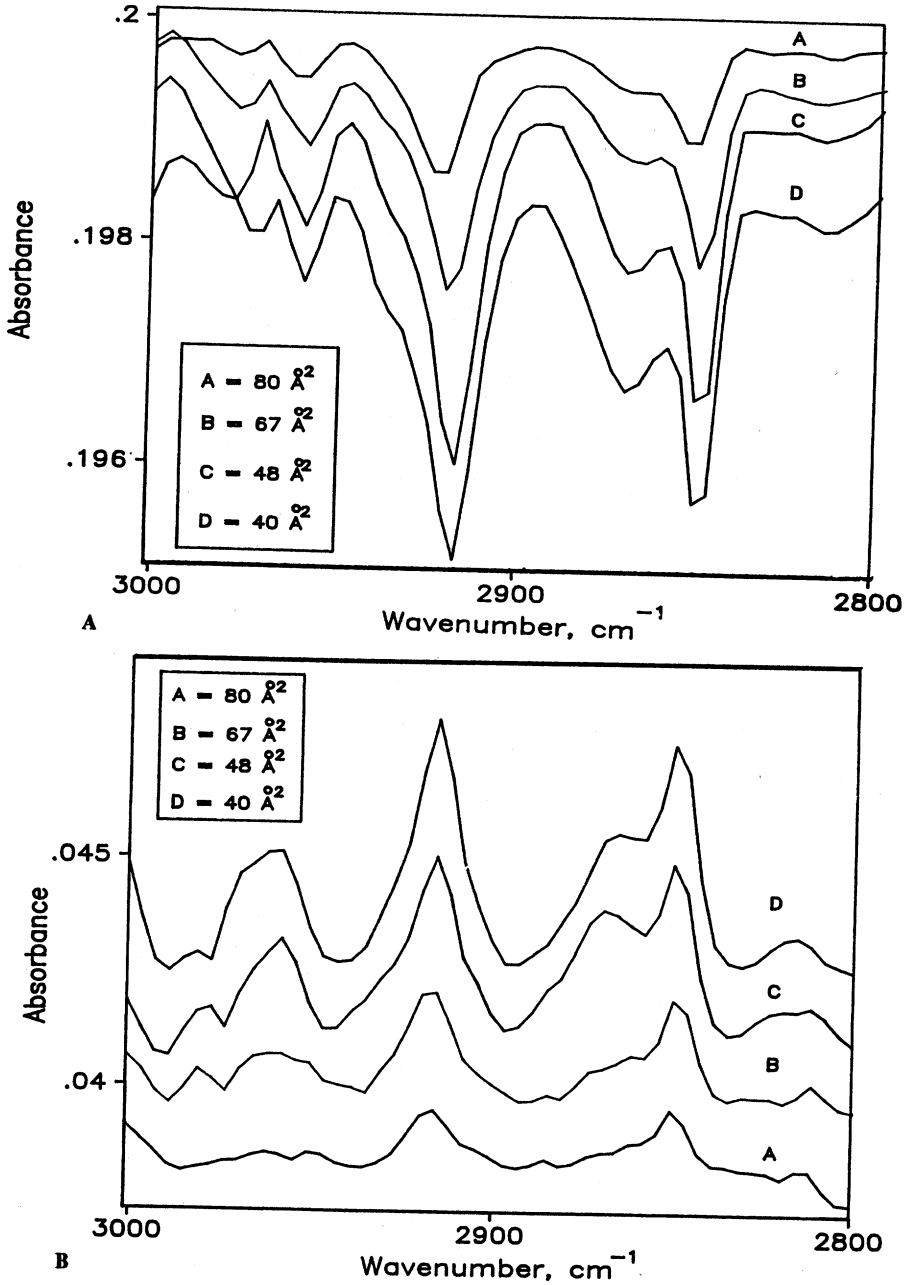

Figure 4. Experimental spectra of the DPPC monolayer at differing molecular areas. The angle of incidence of the incoming radiation was 60° relative to the surface normal. Figure 4A (top) shows s-polarized spectra; Figure 4B (bottom) shows p-polarized spectra. The precise monolayer molecular areas at which each spectrum was obtained are given in the figures.

x and y components are negligible due to E field nodes at the interface. For the case of external reflectance at the A/W interface, however, finite values of the E field and, hence, finite absorbances are present in all three orientations (*2*). This complicates the calculation of an overall dipole orientation distribution since all geometric orientations must be considered.

One approach to a solution of this problem was put forward by Hansen (*14*), who derived general equations which express the overall experimental film absorbance in terms of the external reflectance of the substrate. These relations contain within them expressions for the individual anisotropic extinction coefficients in each geometric orientation. Solution of these general equations for the anisotropic extinction coefficients allows for an unambiguous description of the dipole orientation distribution when combined with a defined orientation model.

Recently, this type of analysis has been applied to the experimental spectra of DPPC monolayer films at the A/W interface. A detailed derivation and analysis of these equations as specifically applied to the A/W interface will be presented elsewhere (Dluhy, manuscript in preparation). However, Figure 5 presents the results of the calculations for the average orientation angle of the DPPC hydrocarbon chains as a function of molecular area. The orientation angle was calculated at various molecular areas encompassing the LE, LC, and SC regions of the monolayer pressure-area curve. The results presented in Figure 5 show that throughout the LE and LE-LC regions, the average orientation of the DPPC hydrocarbon chains remains relatively constant, at approximately 50-55° from the surface normal. This value may have two interpretations. First, that the hydrocarbon chains of the monolayer, on average, are tilted by 50-55° from the z geometric direction relative to the A/W interface. Alternatively, because of the standard deviation of the measurements, the measured orientations encompass the so-called "magic angle", 54.74°. At this angle in the assumed orientation distribution function all preferred orientations are averaged, with the result being a completely random, isotropic orientation distribution. The closeness of the calculated orientation angles for the hydrocarbon chains of DPPC in the LE and LE-LC regions to this angle precludes us from specifically choosing one alternative.

As the monolayer is further compressed in the condensed phase beyond 50 $Å^2$ $molecule^{-1}$, the lipid becomes more oriented until it reaches a point where the hydrocarbon chains of the DPPC molecule are tilted at an average angle of 35° relative to the interface normal. This value agrees well with the value of 30° calculated for the average orientational tilt of the hydrocarbon chains of DPPC monolayers in the condensed phase at the A/W interface using synchrotron X-ray diffraction (*15*). In addition, this same value (30-35°) has been calculated for the chain tilt of fully hydrated DPPC multilayers in the gel phase (*16*). Thus, the experimental evidence points to a tightly packed crystal structure for the DPPC monolayer in the condensed phase that is the two-dimensional analog of the three-dimensional low temperature, ordered gel phase structure of the bulk DPPC molecule. However, the IR data suggest that in the expanded and transition phases of the monolayer, DPPC may be in a relatively disordered orientation. This randomness may last until after the LE-LC phase transition, at which point the surface pressure of the condensed monolayer film begins to sharply rise and the hydrocarbon chain becomes more oriented.

Monolayer Films Transferred to Solid Substrates. Historically, the spectroscopic investigation of monolayer physical structure has been performed on films transferred to solid substrates, usually through conventional L-B techniques. A wide variety of methods may then be employed in the study of these films. For example, ultraviolet, circular dichroism, and IR spectroscopy, as well as electron microscopy have been performed on monolayers transferred to quartz (for UV and CD), Ge (for IR), and mica (for EM). While much useful information has been obtained in the study of transferred monolayers, there is always a concern about whether the actual physical process of transfer from a gas-liquid to a gas-solid interface induces a change in the structure of the molecule.

With the development of the external reflectance IR technique for observing monolayers *in-situ* at the A/W interface, we now have the ability, for the first time, to directly compare the structure of the monolayer film at the A/W interface with the monolayer transferred to a solid substrate. In order to determine whether these transfer artifacts occur for the DPPC monolayer, we have studied the structure of DPPC when transferred to Ge ATR crystals. Figure 6 is the pressure-area curve of the DPPC monolayer on which are indicated the points at which film transfer was made. Specific surface pressures of transfer were chosen in order to insure that transferred monolayers were studied in the LE, LE-LC and LC-SC regions, to provide a basis of comparison with the *in-situ* monolayers.

In Figure 7 a comparison is made of the frequency of the CH_2 antisymmetric stretching vibration as a function of molecular area for DPPC monolayer films at the A/W and A/Ge interfaces. As described above, the frequency of this vibration is related to the overall macromolecular conformation of the lipid hydrocarbon chains. For the condensed phase monolayer ($\sim$40-45 Å^2 molecule^{-1}), the measured frequency of the transferred monolayer film is virtually the same as that of the *in-situ* monolayer at the same molecular area, indicating a highly ordered acyl chain, predominately all-trans in character. For LE films as well as films transferred in the LE-LC phase transition region, however, the measured frequency appears independent (within experimental uncertainty) of the surface pressure, or molecular area, at which the film was transferred. The hydrocarbon chains of these films are more disordered than those of the condensed phase transferred films. However, no such easy comparison can be made to the *in-situ* monolayers at comparable molecular areas. For the LE monolayers (> ca. 70 Å^2 molecule^{-1}), the transferred monolayers are more ordered than the *in-situ* film. In the LE-LC phase transition region ($\sim$55-70 Å^2 molecule^{-1}), the opposite behavior occurs.

The ATR spectra of the transferred monolayer may also be used to calculate the orientation distribution of the hydrocarbon chains in the transferred film. In this case, the dichroic analysis of the polarized ATR spectra proceeds from well-known principles; a detailed analysis has been presented elsewhere (*17*).

The results for the calculation of the orientation distribution for the hydrocarbon chains in the transferred monolayer films are presented in Figure 8. As is the case with the orientation distribution of the *in-situ* monolayers, the transferred films have a similar tilt angle in the expanded and phase transition regions. For the transferred monolayer, however, the tilt angle is in the range 35-40° from the surface normal, a much more oriented monolayer than the calculations indicate for the *in-situ* film (Figure 5). Figure 8 also shows that the condensed phase transferred monolayers are more oriented than those films transferred in the LE and LE-LC

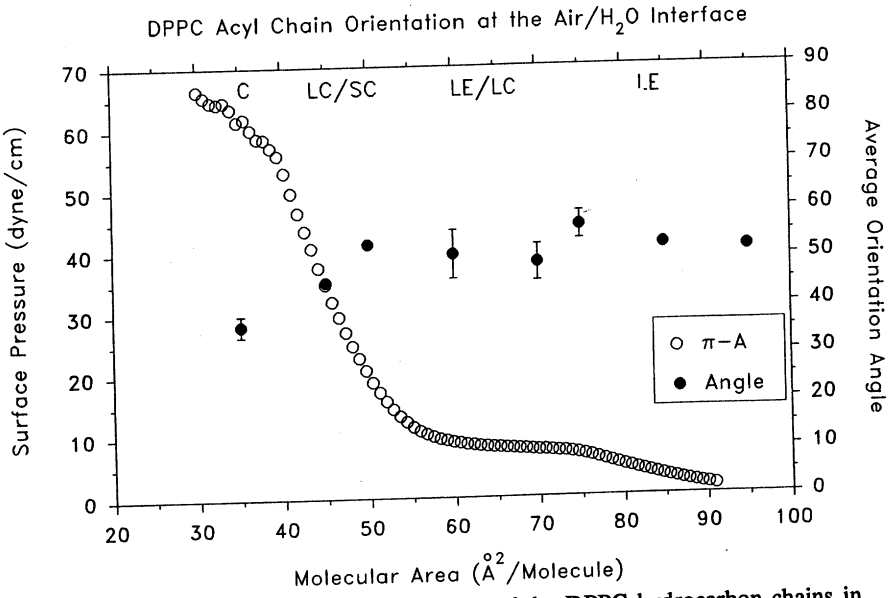

Figure 5. The average angle of orientation of the DPPC hydrocarbon chains in the in-situ film at the A/W interface as a function of the monolayer molecular area (solid circles). The pressure-area curve of DPPC (open circles) is superimposed on the figure.

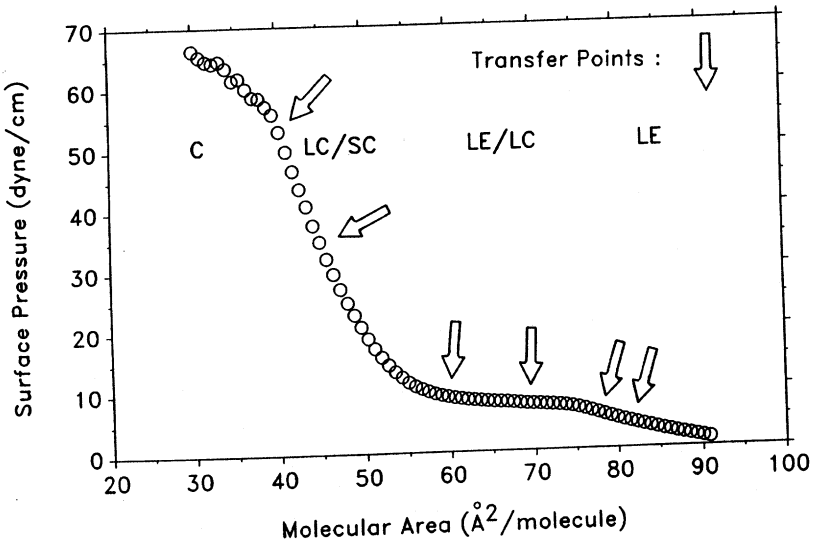

Figure 6. The points along the pressure-area curve of DPPC at which monolayer transfers onto Ge ATR crystals were made.

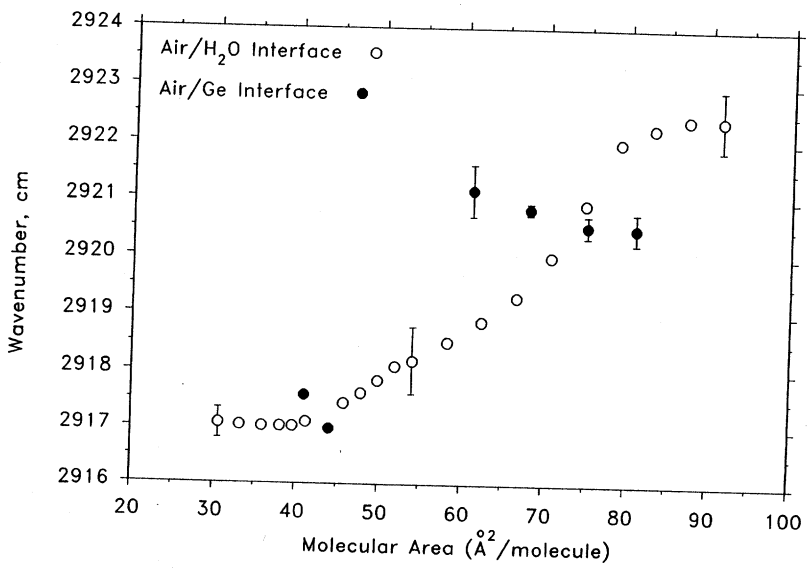

Figure 7. The calculated frequency of the CH_2 antisymmetric stretching vibration in the transferred DPPC monolayer films (solid circles) plotted against the molecular area at which the film was transferred. The frequency of this vibration for the in-situ monolayer film at the A/W interface is superimposed on the plot (open circles).

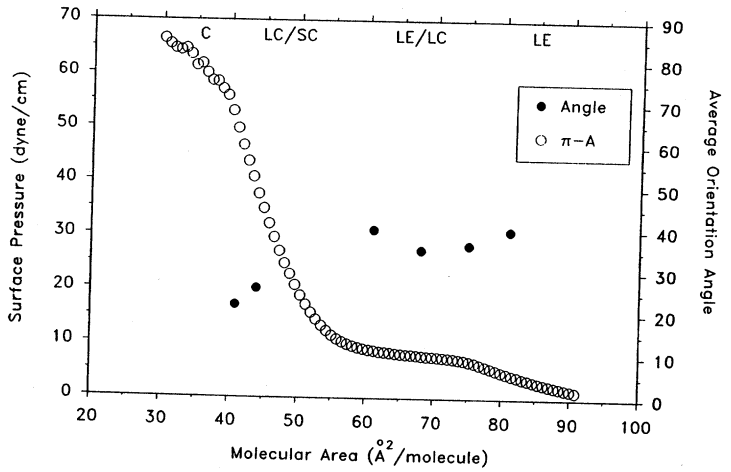

Figure 8. The average angle of orientation of the DPPC hydrocarbon chains in the transferred monolayer films on Ge ATR crystals as a function of the monolayer molecular area (solid circles). The pressure-area curve of DPPC (open circles) is superimposed on the figure.

regions, as well as being more oriented than the *in-situ* monolayer films at similar molecular areas.

Conclusion

Modern methods of vibrational analysis have shown themselves to be unexpectedly powerful tools to study two-dimensional monomolecular films at gas/liquid interfaces. In particular, current work with external reflection-absorbance infrared spectroscopy has been able to derive detailed conformational and orientational information concerning the nature of the monolayer film. The LE-LC first order phase transition as seen by IR involves a conformational gauche-trans isomerization of the hydrocarbon chains; a second transition in the acyl chains is seen at low molecular areas that may be related to a solid-solid type hydrocarbon phase change. Orientations and tilt angles of the hydrocarbon chains are able to be calculated from the polarized external reflectance spectra. These calculations find that the lipid acyl chains are relatively unoriented (or possibly randomly oriented) at low-to-intermediate surface pressures, while the orientation at high surface pressures is similar to that of the solid (gel phase) bulk lipid.

It has also proven possible to directly compare the structure of the monolayer film at the A/W interface with the structure of the monolayer film transferred onto a solid substrate using conventional L-B methods. For DPPC monolayer films transferred to Ge ATR crystals at low-to-intermediate pressures, the transferred monolayer films have a constant conformational order independent of the transfer pressure, and an orientational distribution that is more ordered than that of the *in-situ* monolayer. For those monolayer films transferred at high surface pressures, the hydrocarbon chains have a similar conformational order but are more oriented than the *in-situ* monolayer at the same surface pressure,

Given the ubiquitous nature of interfacial thin films, and the current revival of interest in Langmuir film balance technology, we believe that the results and new techniques described in this chapter will find applications in analytical, physical, and biological chemistry.

Abbreviations Used

A/W	air-water interface
ATR	attenuated total reflectance
C	collapsed
CD	circular dichroism
DPPC	1,2-dipalmitoyl-*sn*-glycero-3-phosphocholine
EM	electron microscopy
FT-IR	Fourier transform infrared
Ge	germanium
IR	infrared
L-B	Langmuir-Blodgett
LC	liquid-condensed
LE	liquid-expanded
SC	solid-condensed
UV	ultraviolet

Acknowledgment

This work was supported by the Public Health Service through National Institutes of Health grant GM40117 (RAD).

Literature Cited

1. Swalen, J.D., Allara, D.L., Andrade, J.D., Chandross, E.A., Garoff, S., Israelachvili, J., McCarthy, T.J., Murray, R., Pease, R.F., Rabolt, J.F., Wynne, K.J., and Yu, H. Langmuir 1987, 3, 932.
2. Dluhy, R.A. J. Phys. Chem. 1986, 90, 1373.
3. Dluhy, R.A., Mitchell, M.L., Pettenski, T., and Beers, J. Appl. Spectrosc. 1988, 42, 1289.
4. Mitchell, M.L. and Dluhy, R.A. J. Am. Chem. Soc. 1988, 110, 712.
5. Dluhy, R.A., Reilly, K.E., Hunt, R.D., Mitchell, M.L., Mautone, A.J. and Mendelsohn, R. Biophys. J. 1989, 56, 1173.
6. Hunt, R.D., Mitchell, M.L., and Dluhy, R.A. J. Mol. Structure 1989, 214, 93.
7. Cameron, D.G., Kauppinen, J.K., Moffatt, D., and Mantsch, H. Appl. Spectrosc. 1983, 36, 245.
8. Cornell, D.G. J. Colloid Interface Sci. 1982, 88, 536.
9. Snyder, R.G., Hsu, S.L., and Krimm, S. Spectrochim. Acta, Part A 1978, 34, 395.
10. Snyder, R.G., Strauss, H.L., and Elliger, C.A., J. Phys. Chem. 1982, 86, 5145.
11. MacPhail, R.A., Strauss, H.L., Snyder, R.G., and Elliger, C.A. J. Phys. Chem. 1984, 88, 334.
12. Kjaer, K., Als-Nielsen, J., Helm, C.A., Laxhuber, L.A., and Mohwald, H. Phys. Rev. Letters 1987, 58, 2224.
13. Downing, H.D. and Williams, D. J. Geophys. Res. 1975, 80, 1656.
14. Hansen, W. Symposia of the Faraday Society 1970, 4, 27.
15. Helm, C.A., Mohwald, H., Kjaer, K., Als-Nielsen, J. Europhys. Letters 1987, 4, 697.
16. Tardieu, A., Luzzati, V., and Reman, F.C. J. Mol. Biol. 1973, 75, 711.
17. Cornell, D.G., Dluhy, R.A., Briggs, M.S., McKnight, C.J., and Gierasch, L.M. Biochemistry 1989, 28, 2789.

RECEIVED July 26, 1990